
A comprehensive parametric study of a hybrid islanded microgrid

Hedia Turki, Khadija Ben-Kilani, Mohamed Elleuch

*Université de Tunis El Manar, Ecole Nationale d'Ingénieurs de Tunis, LR11ES15
Laboratoire des Systèmes Electriques, 1002, Tunis, Tunisie
turkihed61@gmail.com, khadijakilani@yahoo.fr, melleuch2008@gmail.com*

ABSTRACT. This paper presents a comprehensive parametric study of a hybrid islanded microgrid. The study methodology is based on defining various study cases combining structural and operational parameters of the microgrid. Structural parameters include the type of renewable integrated (wind/PV), the battery set point, AC/DC bus connections, weather conditions, and the loading level. Operating parameters include the battery cycle of charging and the diesel generator operation. The defined cases are assessed for a set of performance criteria: renewable share, cost effectiveness, generator life. The study is further enhanced by a sensitivity analysis of the set criteria to the fuel price. The study cases are the reference islanded Chilien microgrid of Desertores, and a north African site in Tunisia. The study is useful for a preliminary design of a microgrid installation.

RÉSUMÉ. Cet article présente une étude paramétrique globale d'un micro-réseau hybride îloté. La méthodologie de l'étude se base sur la définition de cas d'étude combinant à la fois des paramètres structurels et opérationnels du micro-réseau. Les paramètres structurels incluent le type du renouvelable intégré (éolien /PV), la consigne de la batterie, les connexions au bus AC/DC, les conditions météorologiques et les niveaux de charge. Les paramètres de fonctionnement considèrent le cycle de charge de la batterie et le fonctionnement du générateur diesel. Les cas définis sont évalués pour un ensemble de critères de performance : la part des énergies renouvelables, de l'efficacité des coûts, la durée de vie du générateur. L'étude est renforcée par une analyse de sensibilité des critères établis au prix du carburant. Les cas d'étude sont un micro-réseau référence chilien de Desertores, et un site de l'Afrique du Nord en Tunisie. L'étude est utile pour la conception préliminaire d'un micro-réseau.

KEYWORD: microgrid, islanded operation, wind energy, photovoltaic, diesel generator, dispatch strategy, cost of energy, renewable fraction.

MOTS-CLÉS : micro-réseau, îlotage, énergie éolienne, photovoltaïque, générateur diesel, la météo, stratégie de l'expédition, coût de l'énergie, énergie renouvelable.

DOI:10.3166/EJEE.18.139-158 © Lavoisier 2016

1. Introduction

Remote areas such as islands or mountainous regions are often prevented from utility grid extensions due to inaccessibility or rough reliefs. Other critical loads need to withstand grid failures, such as advanced medical therapies, military stations and refrigeration. For such reasons, added to the dropping cost of renewable generation and energy storage technologies (ABB, 2013), the microgrid concept has become an alternative for supplying electric power to consumers. A key feature of a microgrid is its capability to island itself off from the larger power grid upon faults, and to help integrate distributed renewables into utility-scale resources. Indeed, many examples of microgrid applications have been reported in the literature for supplying islands (Stevens *et al.*, 2013), high altitude villages (Zahnd *et al.*, 2013), and mining sites (Yuan *et al.*, 2014).

Multiple definitions of a microgrid were presented in several works (Dohn, 2011, Asmus, 2013), all agreeing on the main components: distributed generators mostly renewable, loads and storage. Typically, the distributed generators are classified as intermittent or limited power generators. Intermittent generator such as wind and photovoltaic sources should be supported by conventional generators, typically diesel engines, combined heat and power (CHP) or gas turbines (Katiraei *et al.*, 2008) (Shahidehpour *et al.*, 2013). The resulting hybrid structure renders, power management and energy management strategies technical challenges especially in the islanded operational mode of the microgrid (Katiraei *et al.*, 2008). The reliance on intermittent energy without a grid connection necessitates a storage system (Paquette *et al.*, 2012). Diesel generators and storage batteries fall under limited power generators category. Set point operation of each component or the state of charge (SOC) of the batteries is controlled via an interfacing converter. Maximum power point trackers, battery charger and wind turbine speed must be controlled in order govern the entire microgrid (Wang *et al.*, 2013; Jamil *et al.*, 2009).

Generally, performance criteria of a microgrid are essentially sustainability, power quality, economic benefits and the ability of islanded and grid connected operation. However, setting specific operational rules depend on the intrinsic parameters of the microgrid installation site. The dispatcher decision depends on various parameters: the site operating parameters, such as weather conditions, the microgrid configurations, and eventually the desired economic and environmental criteria. Many of the parameters are set at the design stage via a feasibility algorithm taking into account the microgrid components, their technology, their number, their power rating, and their cost.

This paper presents a comprehensive parametric study of a hybrid islanded microgrid. The study methodology is based on the definition of various study cases combining structural and operational parameters of the microgrid. Structural parameters include the type of renewable integrated (wind/PV), the battery set point, the AC/DC bus connections, weather conditions, and the loading levels. Operating parameters include the battery cycle of charging and the diesel generator operation.

The defined cases are assessed for a set of performance criteria: renewable share, cost effectiveness and generator life. The study is further enhanced by a sensitivity analysis of the set criteria to the diesel fuel price. The study tests are the reference islanded Chilean microgrid of Desertores, and a north African site in Tunisia. The results show that the energy mix does not always yield to an optimum microgrid configuration. The study is useful as a preliminary design of microgrids.

2. Methodology

2.1. Microgrid Modeling

The proposed microgrid is a hybrid system containing wind turbines, a diesel generator, a battery bank, residential loads and a main converter as shown in Figure 1.

The renewable energy used in the reference system is wind energy. It is introduced in the model with an availability corresponding to the geographic site where the micro grid is implemented. The wind profile is generated from monthly average data. A renewable fraction can further be calculated. This criterion refers to the renewable portion out of the total electrical production. Several metrics may be used to define the renewable fraction penetration: based on the instantaneous peak, the load peak, the system capacity, or penetration based on Energy (Lilienthal, 2007). Such metrics lead to different renewable penetration levels for the same system as shown in Table 1.

In this paper, the renewable share noted f_{ren} is estimated based on the annual average share of the renewable according to:

$$f_{ren} = \frac{E_{ren}}{E_{tot}} \quad (1)$$

Where E_{ren} (kWh) is the renewable annual electrical production, and E_{tot} (kWh) is the total annual electrical production.

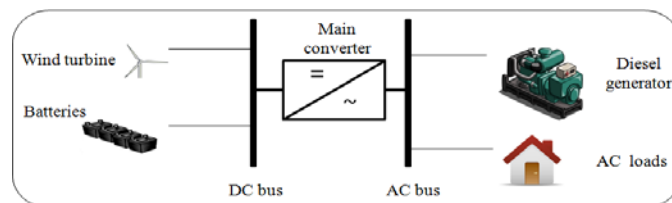


Figure 1. The proposed microgrid general structure

Table 1. Renewable penetration (Lilienthal, 2007)

	Wind	Solar
Peak Instantaneous Penetration	25%	15%
Penetration Based on Peak Load	10%	10%
Penetration Based on System Capacity	6.67%	6.67%
Penetration Based on Energy	5%	3%

Incorporating renewable energy in a power production system influences the system cost and essentially lowers the final cost of energy. Indeed, increasing the renewable fraction reduces the fuel consumption, yielding environmental and economic benefits. The cost of energy (COE) is defined as the average cost of 1 kWh of useful electrical energy produced by the system, and is computed by Equation (2) as:

$$COE = \frac{C_{ann\ opt}}{E_{primAC}} \tag{2}$$

Where $C_{ann\ opt}$ (\$/yr) is the total annual cost of the system, and E_{primAC} (kWh/yr) is the AC primary load served.

The backup generator used in the reference system is a diesel generator, used to overcome power outages due to unavailability of wind power, or when the battery is discharged. Its operation can be scheduled, if needed, specifying the times of the day and year during which the generator must or not operate. In the present study, the diesel generator operates based on the electrical demand, to satisfy unsupplied load.

The conventional generator life (R_{gen}) in a microgrid is a parameter equally significant for the choice of the dispatch strategy. It is specified in terms of yearly operating hours. The number of years that a generator will last is defined as the operational life, calculated according to Equation (3):

$$R_{gen} = \frac{R_{gen,h}}{N_{gen}} \tag{3}$$

Where $R_{gen,h}$ (hr), is the generator lifetime and $N_{gen}(hr/yr)$ is the number of hours the generator operates during one year.

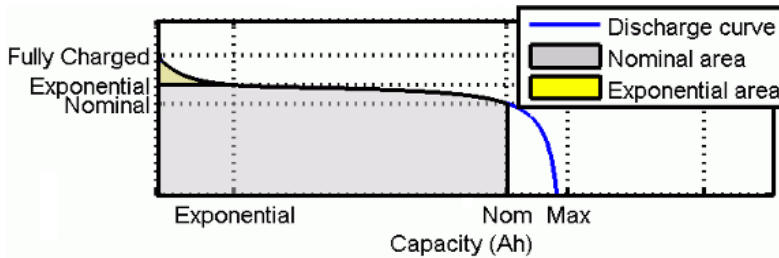


Figure 2. Typical discharge characteristic of a battery

Adding batteries to the microgrid enhances maximizing renewable contribution. Batteries promote efficient use of intermittent energy, improve system control and facilitate the balance between demand and production (San Martin, 2011). A typical discharge characteristic of a battery is presented in Figure 2. The first section represents the exponential voltage drop when the battery is charged. The second section is the nominal area where energy can be extracted from the battery before the voltage drops below the battery nominal voltage. Finally, the third section presents the total discharge of the battery, when the voltage drops rapidly.

The performance of a battery bank can be measured by several parameters. We can choose the autonomy and the life of the battery bank. The autonomy, expressed in hours, is the maximum time that the battery can continuously release energy. It is defined as the ratio of the battery bank size to the electric load, and calculated by Equation (4)

$$A_{batt} = \frac{N_{batt} \times V_{nom} \times Q_{nom} \times (1 - q_{min}/100) \times (24 \text{ h/d})}{L_{prim,ave} \times (1000 \text{ wh/kwh})} \quad (4)$$

Where N_{batt} is the number of batteries in the battery bank, V_{nom} (V) is the nominal voltage of a single battery, Q_{nom} (Ah) is the nominal capacity of a single battery; Q_{min} (%) is the minimum state of charge of the battery bank, and $L_{prim,ave}$ (kwh/d) is the average primary load. The battery life, expressed in years, is the time that the battery can last before it is damaged by use or age, computed by Equation (5):

$$MIN\left(\frac{N_{batt} \times Q_{lifetime}}{Q_{thprt}}, R_{batt,f}\right) \quad (5)$$

Where

- R_{batt} : battery bank life (yr);
- N_{batt} : number of batteries in the battery bank;
- $Q_{lifetime}$: lifetime throughput of a single battery (kWh);
- Q_{thprt} : annual battery throughput (kWh/yr);
- $R_{batt,f}$: battery float life (yr);

The parameter lifetime throughput is defined by Equation (6)

$$Q_{lifetime} = f \times d \times \left(\frac{q_{max} \times V_{nom}}{1000 \text{ W/kW}}\right) \quad (6)$$

Where

- f: the number of cycles to failure;
- d: the depth of discharge (%);
- q_{max} : the maximum capacity of the battery (Ah);
- V_{nom} : the nominal voltage of the battery (V);

The float life of the battery is the maximum length of time that the battery will last before it needs replacement, regardless of how much or how little it is used. This limitation is typically associated with the damage caused by corrosion in the battery, which is strongly affected by ambient temperature.

The battery operation and control are based mainly on the SOC and the set point SOC. The SOC indicates to the system if the battery needs to be charged or how much energy it can absorb in surplus. The operation is also related to the battery set point state of charge. If a set point state of charge is applied, the system will not stop charging the battery until it reaches the set point SOC. The latter tends to reduce the number of generator starts and the number of battery charge-discharge cycles that occur throughout the year.

2.2. Case study methodology

The proposed study is based on a comparative parametric analysis of different operating scenarios of the microgrid. The idea is to vary the diesel price, the set point of the SOC, the weather conditions, the dispatch strategy and the system configuration or components, and to see their impact on renewable fraction and cost of energy. Table 2 summarizes the different considered scenarios. A comparison is made between Chili and Tunisia with the same microgrid configurations. The weather and diesel price are not the same in both countries. Also, Photovoltaic-Diesel (PVD) and Wind-Photovoltaic-Diesel (WPVD) systems were used in addition to the original Wind-Diesel (WD) system in both countries. In Tunisia three sites were tested: Tunisia Capital, Tunisia North and Tunisia South. Meteorological data is obtained from the National Aeronautics and Space Administration (NASA) website. The cases listed in Table 2 are compared with respect to the following economic and technical criteria: renewable fraction cost of energy and generator life.

Table 2. Study cases definition

Microgrid Site		Load level		Microgrid Configuration				Dispatch strategy	
		High $\mu G2$	Low $\mu G1$	WD	PVD	WPVD	PV AC side	CC	LF
Chili	Auteni	x		x	x	x		x	x
	Imerquina		x	x	x		x	x	x
Tunisia	North	x		x	x	x		x	x
			x	x	x		x	x	x
	Capital	x		x	x	x		x	x
			x	x	x		x	x	x
	South	x		x	x	x		x	x
			x	x	x		x	x	x

WD: Wind-Diesel; PVD:Photovoltaic-Diesel; WPVD:Wind-Photovoltaic-Diesel.

2.3. Microgrid operation

The microgrid operation is based on a dispatch strategy via a set of rules that govern the renewable generators, the diesel generator, and battery bank. For the battery bank, two dispatching strategies are used: load following (LF) and cycle charging (CC). Under the load following strategy the generator produces only the power that satisfies the demand, if needed. This strategy is used when there is a lot of renewable production that exceeds sometimes the load. Under cycle charging strategy the diesel generator operates at full capacity and the surplus power charges the battery bank until it reaches the specified set point SOC. This strategy is used when there is a little or no renewable power.

2.3.1. Study case 1: Chili microgrid

The first study system is based on the Desertoires Island example in Chili (Stevens *et al.*, 2013). It consists of a group of eight generation sites supplied all with autonomous microgrids with a configuration based on Wind-Diesel generation. The residential load demand is different from one site to another, so the system components sizing is adjusted. We have chosen to study the Auteni site with the highest load demand and Imerquina site with the lowest load demand as shown in Table 3. They are denominated μ G1 and μ G2 respectively.

The dispatch strategy chosen in optimization results for μ G1 in all varying geographic sites and system designs is the cycle charging strategy. μ G1 design presents a relatively low renewable fraction, always lower than 45%. As shown in Figure 3, the diesel generator starts working at full capacity 25kW, in January 8, at 5.30 pm to meet the load since the total production is not satisfying the demand. The SOC in this case has increased from 77% to 80% at 7.30 pm thanks to the surplus of power. On January 9, when the SOC reaches 35% the diesel generator starts operating at 3.30 pm and stops on January 10 at 6.30 am when the SOC has exceeded 80%, which is the value of the set point programmed initially.

Table 3. Studied microgrid detailed design

Components	μ G1 load 175 kWh/d		μ G2 load 16.8 kWh/d	
	Quantity	Unit size	Quantity	Unit size
Wind turbine	2	7.5kW	1	3.5kW
Diesel generator	1	25kW	1	5kW
Battery	96	3kWh	24	3kWh
Converter	3	5kW	1	5kW

A sensitivity analysis is performed on the SOC by varying this parameter from 30% to 80% with increments of 10%. The Results show that the renewable fraction is slightly sensitive to the SOC.

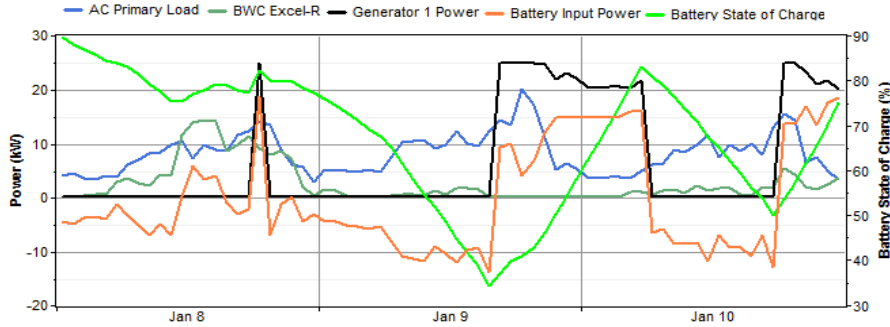


Figure 3. Chili Auteni microgrid operation under CC dispatch strategy

The CC and the LF dispatch strategies are compared for $\mu G1$ and the results are summarized in Table 4. Both strategies show comparable renewable share as indicated by the *fren* values, whereas the LF gave higher COE than the CC strategy. The generator lifetime (*Rgen*) under CC was higher than under the LF strategy. This parameter expressing the diesel generator life validates the choice of the CC strategy as optimal solution.

Table 4. Comparison between CC and LF dispatch strategies for $\mu G1$

Chili		Fren		COE (\$/kWh)		Rgen (yr)	
Sites	Configuration	CC	LF	CC	LF	CC	LF
Auteni $\mu G1$	WD	0.41	0.45	0.764	0.906	7.46	3.41
	PVD	0.25	0.27	0.867	1.054	4.8	2.56
	WPVD	0.34	0.36	0.827	1.001	5.27	2.89
Imerquina $\mu G2$	WD	0.8	0.85	1.212	1.257	46.2	19.9
	PVD	0.56	0.59	1.271	1.469	22.3	7.71

For $\mu G2$, the design presents an important renewable fraction, frequently higher than 60%. The dispatch strategy chosen in optimization results for $\mu G2$ in all varying geographic sites and system designs is the cycle charging strategy. The same sensitivity analysis is performed on the set point of SOC as for $\mu G1$ site. The various system configurations used for $\mu G2$ are WD, PVD and PV on AC side with diesel (PVAC-D). The WPVD configuration was not significant to study because the total renewable installed capacity is equal to 3.5 kW, and only one renewable is source. As shown in Figure 4, the diesel generator operates always at full capacity

5kW but with a considerably low running frequency. During the month of January, it operated only on January 15th and January 22nd for 12 and 13 hours respectively. Moreover, in December the generator has not operated at all as shown in Figure 5. This is due to the low load demand which can be often satisfied by the renewable production and the storage device. This also explains the increased generator life which was worth 46.2 yr.

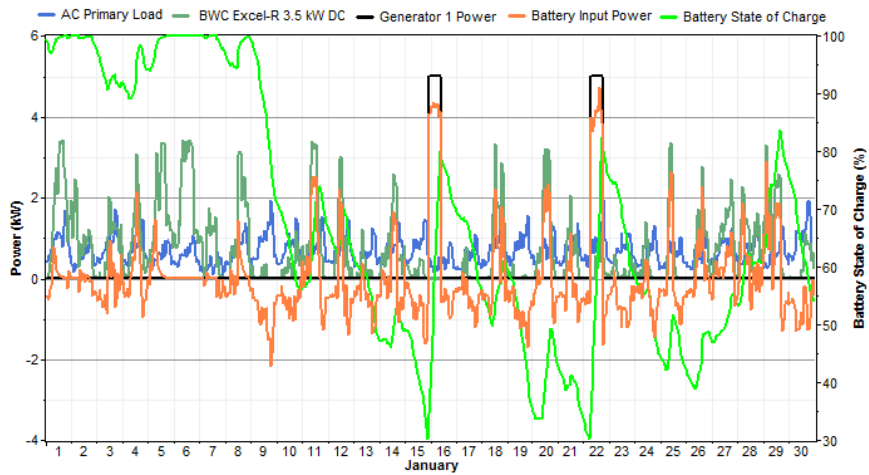


Figure 4. Chili Imerquina microgrid operation under CC dispatch in January

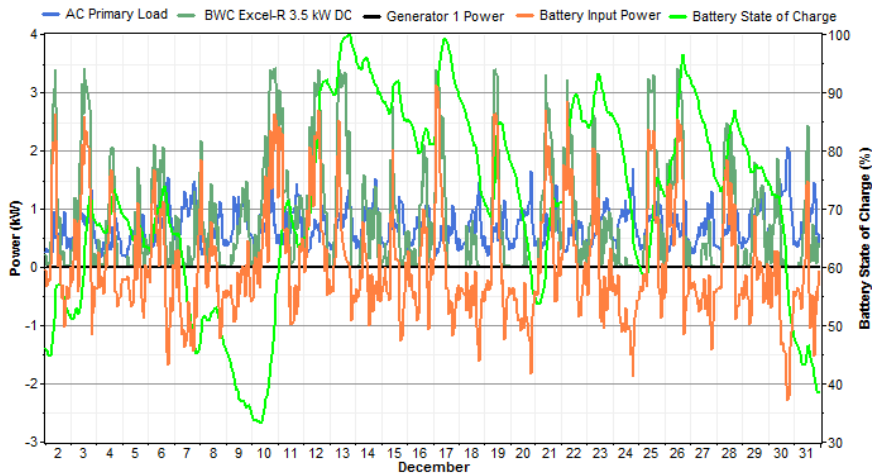


Figure 5. Chili Imerquina microgrid operation under CC dispatch strategy in December

The LF strategy results for $\mu G2$ are summarized in Table 4. Comparing the two strategies, the LF presents a bit higher renewable fraction but a higher COE and a considerably lower generator life as shown in Table 5. The generator life in $\mu G2$ is even higher than presented in $\mu G1$ thanks to the lower number of starts. Thus the CC choice for the optimized system is justified.

2.3.2. Study case 2: Tunisia microgrid

The same configurations denoted $\mu G1$ and $\mu G2$ are considered in the south of Tunisia, the results are summarized in Table 5. The adherence between results emphasizes the impact of the dispatch strategy and the load level.

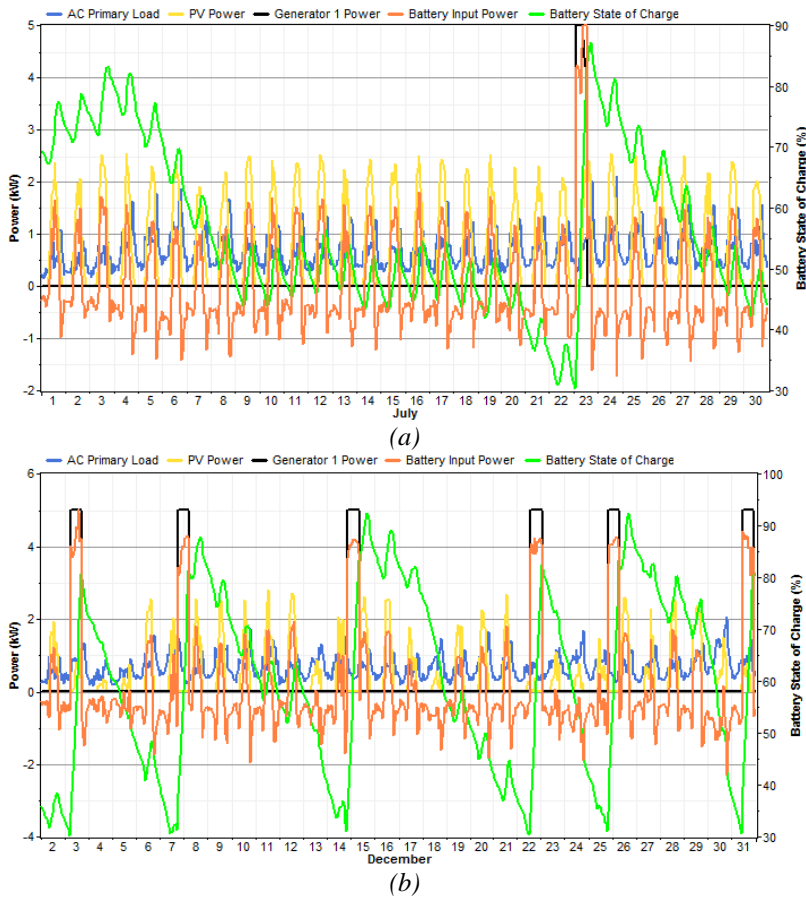


Figure 6. South Tunisia $\mu G2$ operation under CC dispatch strategy.
(a) July; (b) December

The μ G2 with PV-D in south Tunisia system has presented the highest renewable fraction of the three microgrids implemented in Tunisia. It is worth 0.71 under the CC dispatch strategy. It is noted that despite that the renewable fraction under LF strategy, 0.74 is a bit higher; the generator life was much shorter, that is 11.9 years compared to 34.1 years under the CC dispatch strategy. The sunny south of Tunisia seems to promote this type of small scale systems.

For the month of December, Figure 6 shows that the diesel generator operated 6 times, compared to only once during the month of July. On average, the diesel generator operated 3 times a month. With the PV system, the solar production is regular or almost uniform especially during the summer. This explains why the battery SOC presented the same variations shape as the PV power (Figure 6).

Table 5. Comparison between CC and LF dispatch strategies for μ G2

South Tunisia		Fren		COE (\$/kWh)		Rgen (yr)	
Sites	Configuration	CC	LF	CC	LF	CC	LF
μ G1	WD	0.17	0.19	1.003	1.246	4.43	2.26
	PVD	0.3	0.33	0.894	1.126	6.29	2.62
	WPVD	0.23	0.25	0.972	1.227	4.75	2.32
μ G2	WD	0.29	0.33	1.564	1.910	13.6	4.73
	PVD	0.71	0.74	1.217	1.347	34.1	11.9

As shown in Figure 7(a), the diesel generator starts working on January 13th at full capacity when the SOC reached 30%. When the PV production has risen to 2.25 kW the diesel generator has decreased its output power to 3.75 kW. The surplus power induced by the PV should serve the load directly from the AC side.

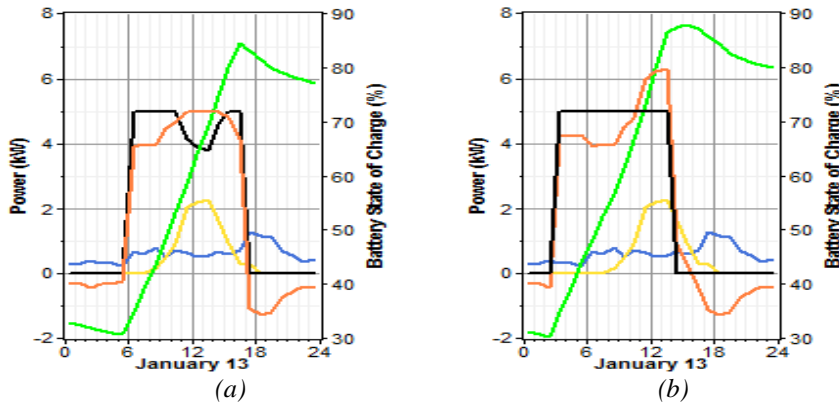


Figure 7. Comparison between PV on the DC side connection and PV on the AC side connection. (a) AC side; (b) DC side

For the PV site, it is worth comparing its connection to the AC side or to the DC side of the converter. Figure 8 shows that when the PV is connected to the DC side, the operation of the diesel is slightly different. As shown in Figure 8(b) when the diesel generator starts, it operates always at full capacity and the surplus power is injected directly to the battery from the DC side.

2.4. Excess electricity

An important aspect of isolated microgrids operation is the excess electricity management. This excess of electric power may result when the load is totally satisfied and the battery is fully charged. Energy balancing necessitates a dump load in the system design to absorb the excess energy. Figure 8 demonstrates a day of operation with excess electricity, on July 26 in Auteni: the battery was fully charged, the wind turbine operating at maximum rating, the load was satisfied and the surplus had no way to be evacuated. The excess electricity averaged to 0.77%/yr, and instantly it reached about 10 kW as shown in Figure 9.

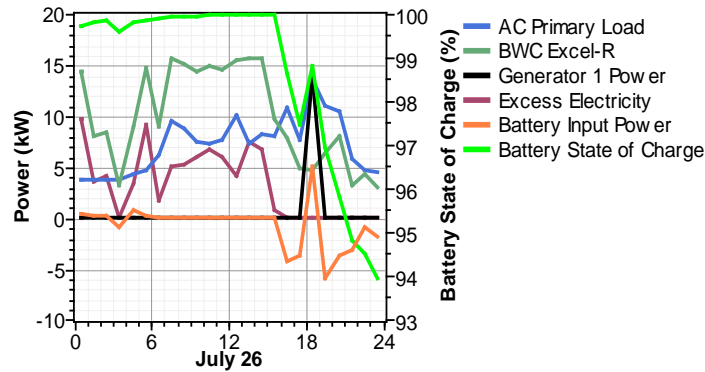


Figure 8. Excess electricity for $\mu G1$ in Auteni site on July 26

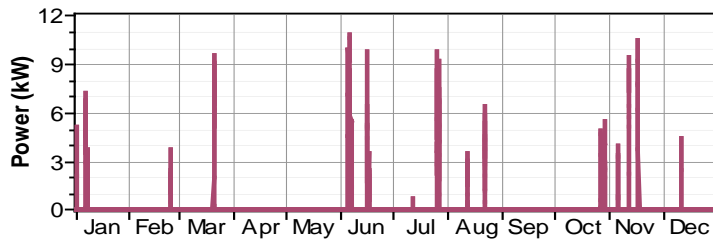


Figure 9. Excess electrical power in $\mu G1$ in Auteni site

In Imerquina (μ G2), the excess electricity was worth 9.95%/yr and reached instantaneous 3 kW as shown in Figure 11(a). As it can be seen in Figure 10(a), the battery input power is zero while there is an amount of energy that had no evacuation process. For μ G2 implemented in south Tunisia, the excess electricity amount was much significant as illustrated in Figures 11(b)-11(c). It is worth 0.05%/yr for the PV connected on the DC side, and 0.02%/yr for the AC side connection. It can reach an instantaneous peak of 1kW. As shown in Figure 10(b), on January 7, an excess energy began to occur around midday when the sun was high. The PV power was higher than the load demand, and the SOC was almost 95 %. The excess electricity vanished when the sun proceeded to set.

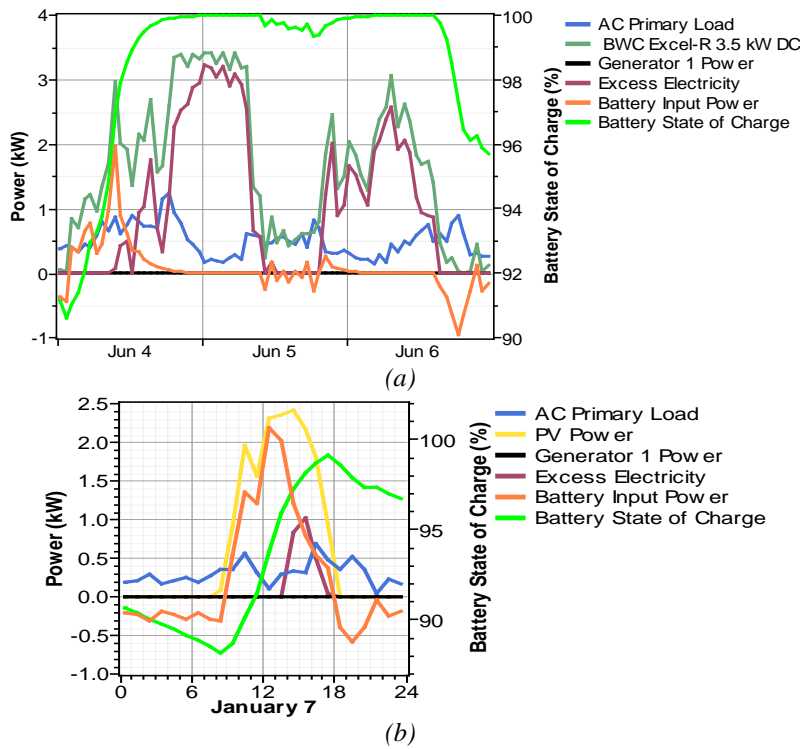


Figure 10. Excess electricity for μ G2 in (a) Imerquina WD, and (b) Tunisia PVD (DC side)

This information is helpful for the operation management of the isolated microgrid. To overcome this problem, dump loads may be placed to absorb the excess flow of energy. Dump loads can be simply heater resistors or light bulbs. A supplementary control is then intended in the future system design to set and size the dump loads. Another alternative to be discussed is to inject that surplus to the grid.

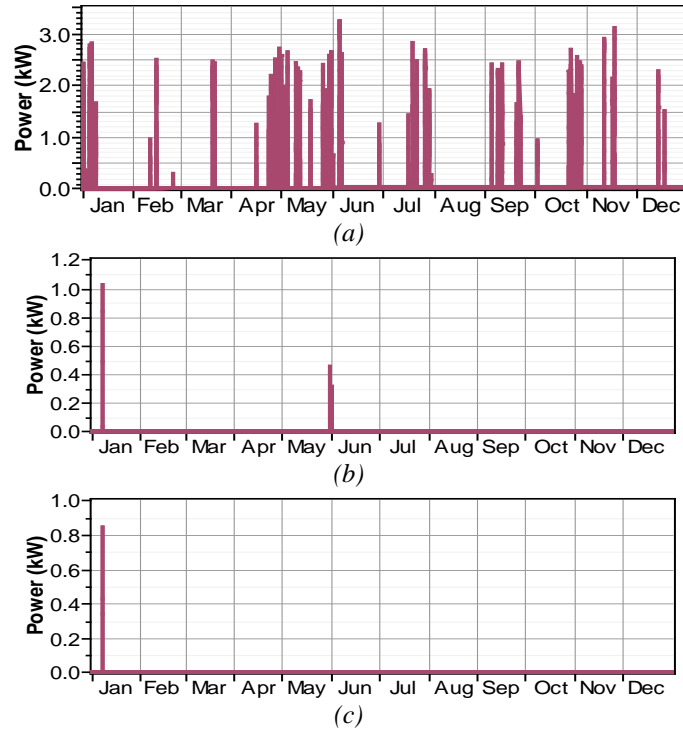


Figure 11. Excess electricity for (a) μ G2 Imerquina, (b) South Tunisia μ G2 PV DC side, and (c) South Tunisia μ G2 PV AC side

When substituting wind turbines by solar panels in South Tunisia, the total PV production is lower than wind production. The renewable participation of wind is higher than solar due to climate criteria. For μ G1, wind production was worth 33534 kWh/yr in Chili. After modifying the system to PVD, the solar production was worth 22912 kWh/yr in Tunisia. The same applies to μ G2 where the production of wind and solar were worth 6565 kWh/yr and 5337 kWh/yr respectively. So comparing WD system and PVD system, the issue of excess electricity is much less problematic for PVD systems.

2.5. Battery operation

The cycle charging dispatch strategy follows the charging-discharging cycle of the battery. For the μ G1 in Auteni, there are 4 battery strings each of 24 batteries presenting an autonomy of 27.6 hours and their expected life is 15.5 years. As shown in Figure 12(a), the battery bank is 80% charged at a frequency of 14% and fully (100%) charged at a frequency of 4%. As it can be seen, the SOC can overshoot the set point of SOC (80%) specified since the battery bank should absorb

a surplus until 100% full, based on need. However in Imerquina site $\mu G2$, the battery bank is more frequently fully charged as shown in Figure 12(b) at a frequency of 14%, and it is between 70%-90% charged at a frequency of almost 8%. For $\mu G2$, the autonomy is of 72 year and the expected life is 20 years.

When substituting the wind energy by solar energy, the battery bank holds its state of charge between 60% and 80%, almost the same behavior as for $\mu G1$ (Figure 12(c)). The autonomy is 27.6 hours and the expected life is 14.7 years. For $\mu G2$, the SOC is almost uniformly spread as shown in Figure 12(d). The autonomy is equal to 72 hours and the expected life is 20 years. The depth of discharge reaches low values in this case and the battery has frequently a full charge-discharge cycle.

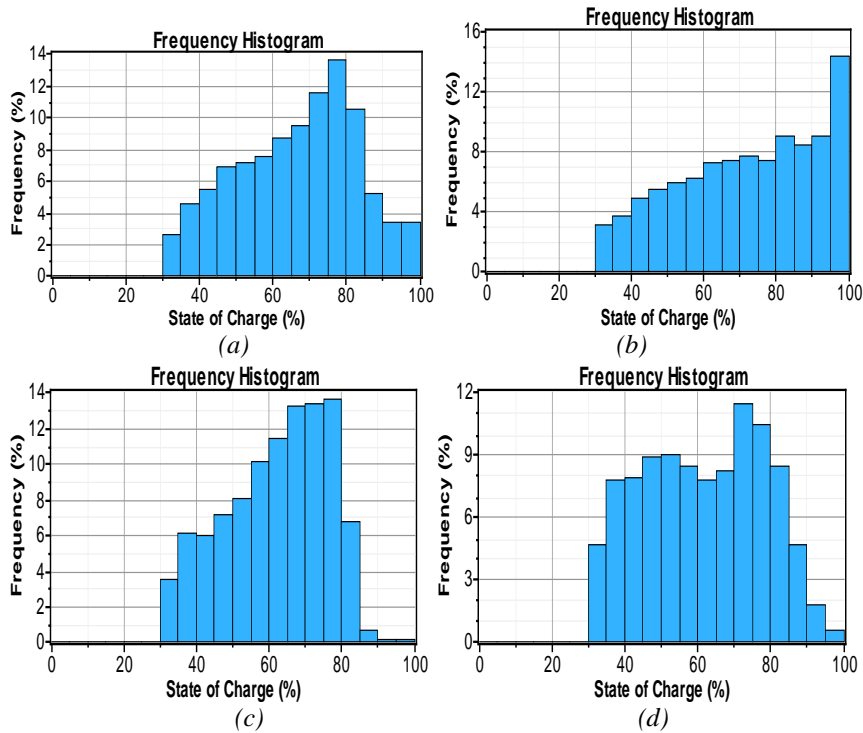


Figure 12. Frequency histogram of battery state of charge for (a) $\mu G1$ WD in Auteni, (b) $\mu G2$ in Imerquina, (c) $\mu G1$ PVD in South Tunisia, and (d) $\mu G2$ in South Tunisia

2.6. Sensitivity to diesel price

A sensitivity analysis is performed on the unitary diesel price. The diesel price is worth 0.933 \$/L and 1.23 \$/L, in Chili and Tunisia respectively. We vary the price from 0.1 \$/L to 2 \$/L with 0.1 increments. The results presented in Figure 13 show

that the renewable fraction is almost constant or slightly sensitive to the diesel price. In Imerquina, Chili, with the WD configuration, the renewable fraction stabilizes when the diesel price reaches 0.2 \$/L. In South Tunisia, for WPVD the optimum system is the PVD until the diesel price reaches 0.6\$/L. Beyond that, the optimum becomes the WPVD. For the WD configuration, it is not economic to integrate renewable production, until the diesel price decreases down to 0.6 \$/L.

On the other hand, for the μ G2 WD configuration in South Tunisia, the renewable fraction is zero until the diesel price reaches 1\$/L. Thus the optimum system is the diesel battery configuration until the diesel price exceeds 1\$/L. The optimum system depends on the COE. In South Tunisia, the COE is considerably higher with WD configuration and is worth 1.564 \$/kWh. It is the highest value in all cases since the wind availability in this site does provide good wind energy integration. So the variation starts to be marked when the system configuration does not fit with the wind or the sun availability in the site. The dependency becomes apparent when the same system is implemented in very different climate conditions. For example, in Figure 13 when comparing Chili μ G2 WD and South Tunisia μ G2 WD, the renewable fraction increases rapidly to 0.8 in the first case while it reaches 0.29 very slowly in the second case, function of the diesel price.

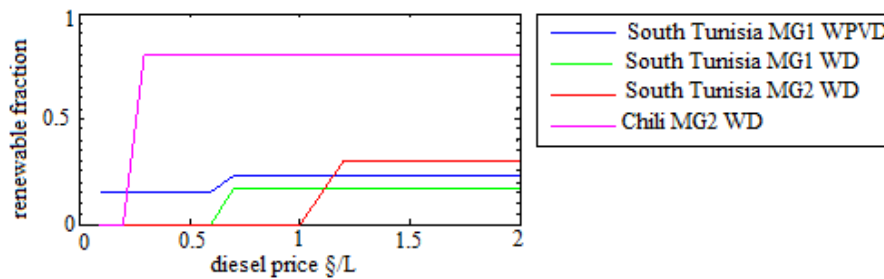


Figure 13. Renewable fraction sensitivity to diesel price

2.7. System design and weather condition

The renewable fraction in a microgrid operation depends on the resources availability in the geographic site. Chili is windy compared to South Tunisia where the annual average speeds are worth to 5.8m/s and 3.9m/s respectively. Moreover, the annual average radiations are equal to 3.72 kWh/m²/d and 5.13 kWh/m²/d in South Tunisia. As shown in Table 5 for μ G1 Chili, the renewable fraction has decreased from 0.41 for wind integration, to 0.25 for PV system integration. On the contrary, it has increased from 0.17 (wind) to 0.31(PV) in South Tunisia. Going down Table 5, it is depicted that the renewable fraction decreases in Tunisia with the same WD system configuration especially in the south where it fell from 0.41 to 0.17.

As shown in Table 6 for $\mu G2$, the renewable fraction is considerably high compared to $\mu G1$, because the daily demand is lower. Going down Table 7, for WD configuration, the renewable fraction decreases from 0.8 to 0.29 in South Tunisia. When introducing photovoltaic, the renewable fraction decreases from 0.81 to 0.56 in Chili and increases from 0.29 to 0.71 in South Tunisia.

Table 5. $\mu G1$ renewable fraction in terms of system configuration

$\mu G1$	Configuration		
Sites	Wind-Diesel	PV-Diesel	Wind-PV-Diesel
Chili Auteni	0.41	0.25	0.34
Tunisia Capital	0.33	0.27	0.32
Tunisia North	0.35	0.31	0.33
Tunisia South	0.17	0.31	0.23

Table 6. $\mu G2$ renewable fraction in terms of system configurations

$\mu G2$	Configurations		
Sites	Wind-Diesel	PV-Diesel	PV AC side-Diesel
Chili Imerquina	0.8	0.56	0.56
Tunisia Capital	0.7	0.65	0.65
Tunisia North	0.73	0.71	0.72
Tunisia South	0.29	0.71	0.71

These results indicate that the wind and PV mix does not always yield to the optimum configuration. In our case, PV share by half the same renewable participation of the original system with wind turbine. Additional sizing study is required to add a supplementary amount of renewable installed power with respect to an acceptable initial capital cost. In South Tunisia which is a sunny place, the PVD system provided good performance since where PV radiation is more significant in the south than the north.

The renewable share in the generation mix impacts the levelized cost of energy. As shown in Tables 7 and 8, the levelized cost of energy increases when the renewable fraction decreases, which is due to the increased fuel consumption. In Tunisia, the COE is always higher than in Chili due to the difference in fuel price. In addition the COE is sensitive to the system configuration. In the case of the Tunisian Capital site, the same renewable fraction of 0.33 is depicted for $\mu G1$ with WD and WPVD, but the COE was higher with the WPVD configuration. It increased from 0.884 \$/kWh to 0.913 \$/kWh. The total demand is equal to 175kWh/d in both cases.

This difference of 0.029 \$/kWh makes an addition of 5.075 \$/d in detriment of consumers.

For the connection of the PV on the AC side of the converter, and for the case of $\mu G2$, the renewable fraction was the same as the case of the PV DC side connection. However, the COE was a bit lower when the PV was connected to the AC side.

Table 7. COE for $\mu G1$ in terms of system configurations

$\mu G1$	Configurations		
Sites	Wind-Diesel	PV-Diesel	Wind-PV-Diesel
Chili Auteni	0.764	0.867	0.827
Tunisia Capital	0.884	0.907	0.913
Tunisia North	0.867	0.895	0.872
Tunisia South	1.003	0.894	0.972

Table 8. COE for $\mu G2$ in terms of system configurations

$\mu G2$	Configurations		
Sites	Wind-Diesel	PV-Diesel	PV AC side-Diesel
Chili Imerquina	1.212	1.271	1.268
Tunisia Capital	1.328	1.256	1.252
Tunisia North	1.277	1.214	1.209
Tunisia South	1.564	1.217	1.214

3. Conclusion

This paper presented a parametric study of a hybrid isolated microgrid, combining structural and operational parameters, and weather conditions. The study considered two meteorologically different sites: the reference islanded Chilean microgrid of Deserto, and a North African site in Tunisia. Meteorological data is obtained from the National Aeronautics and Space Administration website. The proposed designs are assessed for a set of performance criteria: renewable share, cost effectiveness, generator life. The dependence of renewable share and cost of energy on geographic site, diesel price, dispatch strategy and system configuration was highlighted.

The results show that the type of integrated renewable must be suitable to the site climate. The energy mix does not always yield to the optimum system in terms of cost of energy and renewable fraction. The renewable fraction rises when the system scale decreases, and the cost of energy increases when the renewable fraction is minimized. The dispatch strategy influences the diesel generator life so has an impact on the whole system cost effectiveness.

An issue that should be addressed at the design stage of a microgrid is the excess of electricity management. A dump load ought to be implemented, which imposes an additional initial cost.

The presented study is intended for a preliminary static design of a microgrid. Further aspects need to be investigated, such as power quality, stability, control schemes for voltage and frequency regulation in the islanded microgrid.

Acknowledgements

This work was supported by École doctorale sciences et techniques de l'Ingénieur, École nationale d'ingénieurs de Tunis.

Bibliography

- ABB (2013). Renewable Energy in Microgrids Integration Solutions for Off Grid and Grid Connected Power Systems, <http://www.cleanenergyweek.com.au/dam/cew/presentations/2013-presentations/day-2/off-grid/JUERGEN-ZIMMERMANN-Manager-of-Research-and-Development-ABB-Australia0/JUERGEN-ZIMMERMANN-Manager-of-Research-and-Development-ABB-Australia.pdf>
- Asmus P. (2013). Microgrid Market Opportunities and Challenges. *Microgrid world forum*, March 13, Irvine California
- Dohn R.L. (2011). The business case for microgrids white paper: The new face of energy modernization. Siemens 2011 http://w3.usa.siemens.com/smartgrid/us/en/microgrid/Documents/The%20business%20case%20for%20microgrids_Siemens%20white%20paper.pdf
- Jamil M., Hussain B., Abu-Sara M., Boltryk R.J., Sharkh S.M. (2009). Microgrid Power Electronic Converters: State of the Art and Future Challenges. Universities Power Engineering Conference (UPEC), *Proceedings of the 44th International*, Glasgow
- Katiraei F., Iravani R., Hatziargyriou N., Dimeas A. (2008). Microgrids Management. *IEEE Power and Energy Magazine*, vol. 6, n° 3, May/June, p. 54-65.
- Lilienthal P. (2013). High Penetration of Renewable Energy for Island Grids. <http://www.power-eng.com/articles/print/volume-111/issue-11/features/high-penetrations-of-renewable-energy-for-island-grids.html>
- Paquette A.D., Divan D.M. (2012). Design Considerations for Microgrids with Energy Storage. *Energy Conversion Congress and Exposition (ECCE), IEEE*, p. 1966-1973, September 2012, Raleigh, NC.
- San Martín J.I., Zamora I., San Martín J.J., Aperribay V, Eguía P. (2011). Energy Storage Technologies for Electric Applications. *International Conference on Renewable Energies and Power Quality (ICREPQ'11)*, Las Palmas de Gran Canaria (Spain), 13th-15th April.
- Shahidehpour, Khodayar M.E (2013). Cutting Campus Energy Cost With Hierarchical Control the Economical and Reliable Operation of a Microgrid. *IEEE Electrification Magazine*, vol. 1, September, p. 40-56

- Stevens N., Bergey M. (2013). Wind/Diesel Microgrid Utility Service in Desertores Islands. Wireless Energy and Bergey Windpower, *Microgrid Deployment Workshop 2013*, November 8-9, Cancun, Mexico.
- Wang P., Goel L., Liu X., Choo F.H (2013). Harmonizing AC and DC. *IEEE Power and Energy Magazine*, vol. 11, n° 3, May/June.
- Yuan C., Haj-Ahmed M.A, Illindala M.S. (2014). An MVDC Microgrid for a Remote Area Mine Site: Protection, *Operation and Control. Industry Applications Society Annual Meeting, 2014 IEEE*, Oct. 2014, Vancouver, BC.
- Zahnd A., Clark A. (2013). Optimization of a Solar PV -Wind Turbine Hybrid System for the High-Altitude Village of Chala in the Nepal Himalayas. *HOMER Workhop 2013*. <http://www.microgridconference.com/pdf/zahnd-clark.pdf>

Received: 10 June 2015
Accepted: 7 March 2016